

Article

Bark Morphology and Nutrient Flux in Urban Trees: Investigating Water Absorption and Ion Concentration Dynamics

Marcelle Teodoro Lima ¹, Manuel Enrique Gamero Guandique ² and Kelly Cristina Tonello ^{1,*} ¹ Campus Sorocaba, Federal University of São Carlos, Sao Carlos 18052-780, Brazil; marcellelima@ufscar.br² Campus Sorocaba, São Paulo State University “Júlio de Mesquita”, Jaboticabal 18087-180, Brazil; enrique.gamero@unesp.br

* Correspondence: kellytonello@ufscar.br

Abstract: Urban trees play a pivotal role in mediating the hydrological and nutrient cycles within urban ecosystems, yet the mechanisms by which bark characteristics influence these processes remain underexplored. This study aimed to investigate the impact of the bark morphology—specifically texture, depth, and number of furrows—on the water absorption capacity and to determine the relationship between this capacity and ion concentration in stemflow across various urban tree species. Our findings reveal significant variations in water absorption and ion concentration related to the morphological traits of bark among tree species, highlighting the intricate relationship between bark physical and chemical characteristics and stemflow nutrient composition. Notably, species with furrowed textures, greater depth, and a higher number of furrows demonstrated pronounced differences in ion enrichment in their stemflow. However, a canonical redundancy analysis suggested a low association between bark absorption capacity and ion concentration, indicating the influence of other, possibly external, environmental factors on ion leaching. The results underscore the complexity of nutrient transport mechanisms in urban trees and show a new understanding of tree bark’s ecohydrological roles. This study contributes valuable insights into ecohydrology science and emphasizes the need for further research to unravel the multifaceted influences on nutrient dynamics in urban landscapes.

Keywords: urban hydrology; forest hydrology; bark wettability; ecohydrology; urban ecology; ecosystems services



Citation: Lima, M.T.; Guandique, M.E.G.; Tonello, K.C. Bark Morphology and Nutrient Flux in Urban Trees: Investigating Water Absorption and Ion Concentration Dynamics. *Hydrology* **2024**, *11*, 56. <https://doi.org/10.3390/hydrology11040056>

Academic Editors: Stefanos Stefanidis and Nikolaos Proutsos

Received: 27 March 2024

Revised: 12 April 2024

Accepted: 14 April 2024

Published: 17 April 2024



Copyright: © 2024 by the authors. Licensee MDPI, Basel, Switzerland. This article is an open access article distributed under the terms and conditions of the Creative Commons Attribution (CC BY) license (<https://creativecommons.org/licenses/by/4.0/>).

1. Introduction

Rain plays a crucial role in transferring atmospheric nutrients to the soil in forest ecosystems [1]. The forest structure and species diversity can alter the chemical composition of rain, resulting in differentiated ion concentrations that reach the soil through stemflow [2,3]. In ecohydrology, this process, which connects the canopy with the soil, emerges as a concentrated source of water that influences the spatial distribution of soil moisture [4–6]. Often, its chemical composition presents higher nutrient concentrations compared to open precipitation [7–9]. Recent research indicates that even small volumes of stemflow, relative to incident precipitation, can generate hotspots of water and matter inputs, with significant impacts on subsequent hydrological and biogeochemical processes in soils [10].

In addition to compounds derived from atmospheric deposition, stemflow can transport compounds released by plant tissues, such as organic compounds, gases, and dissolved ions [11–13]. These substances can be absorbed and/or adsorbed by plant surfaces before reaching the soil, a process which is influenced by a complex interaction between abiotic and biotic factors [14–16]. Tree morphology plays a crucial role in stemflow dynamics and nutrient leaching. Factors such as canopy size and shape, trunk diameter, and bark morphological characteristics influence this interaction [17–19]. Bark, a multifunctional

structure that varies between species [20], plays a central role in this process, affecting trunk washing dynamics and dissolved solute exchange [15].

Studies highlight bark's ability to absorb and lose water, emphasizing the importance of wettability and absorption capacity in stemflow flux [13,18,21]. The water storage capacity in bark, often underestimated, directly impacts the geoecology of forest ecosystems, influencing stemflow volume and nutrient leaching [13]. Researchers investigating changes in bark properties and hydrology after controlled burning of *Pinus taeda* and *Quercus montana* in a forest in the eastern United States concluded that the bark structure significantly influences individual tree control in hydrological processes, and they assert that increased bark water retention capacity coupled with accelerated evaporation times can result in reduced water infiltration into the forest soil [22].

The urban environment introduces unique challenges and opportunities for studying these processes. Urban trees are exposed to distinct atmospheric conditions, including pollution and anthropogenic nutrient inputs, which may alter the chemistry of stemflow in ways not observed in non-urban settings. Moreover, the role of urban trees in managing stormwater, improving soil quality, and supporting urban biodiversity highlights the critical need to understand how their physiological and morphological traits influence hydrological and biogeochemical cycles. According to the authors' knowledge, this study is the first to investigate the water absorption capacity of bark in urban trees, aiming to bridge a significant gap in urban ecohydrology.

Given the limited knowledge about the relationship between bark properties and ion concentration in stemflow, the main objective of this research was to investigate the influence of bark morphology on the chemical concentration of stemflow in urban forest species. Specifically, we sought to understand (i) how bark water absorption capacity influences ion concentrations and (ii) how bark physical characteristics correlate with ion leaching. The expected hypotheses were that ion leaching varies substantially among urban species depending on bark properties, both in terms of (1) morphological structure and (2) the water absorption capacity of the bark.

2. Materials and Methods

This investigation was conducted in the urban experimental area of the Federal University of São Carlos, Sorocaba campus, São Paulo, located between the geographic coordinates of 23°17' S and 47°16' W at an average altitude of 580 m. The climate of the region is classified as Cwa [23], with a hot dry temperate climate and hot summer, where the average annual temperature is 22 °C and the average annual precipitation is 1311 mm [24,25]. To avoid contamination of the stemflow, monitoring was carried out on eight (8) tree species that did not have overlapping canopies with neighboring trees. The experiment comprised 3 individuals of each species, totaling 24 individuals, as listed in Table 1.

Table 1. Investigated tree species and their respective diameter at breast height (DBH). Values in parentheses correspond to standard error.

Tree Species	ID	DBH [cm]
<i>Eucalyptus urograndis</i> W. Hill	EU	23.6 (2.9)
<i>Leucaena leucocephala</i> (Lam.) de Wit	LL	19.4 (3.2)
<i>Moquiniastrum polymorphum</i> (Less.) G. Sancho	MP	20.2 (1.4)
<i>Paubrasilia echinata</i> (Lam.) Gagnon, H. C. Lima & GPLewis	PE	18.1 (1.3)
<i>Pinus taeda</i> L.	PT	27.2 (3.7)
<i>Schizolobium parahyba</i> (Vell.) Blake	SP	21.1 (0.8)
<i>Pleroma granulatum</i> (Desr.) Cogn	TG	21.9 (2.5)
<i>Tabebuia roseoalba</i> (Ridl.) Sandwith	TR	20.0 (2.9)

2.1. Hydrological Processes and Ion Concentrations

Rainwater was obtained from three rain gauges made from PVC tubes and fittings (capture area of 254.5 cm² and height of 20 cm) installed in an open area at 1.20 m above the

ground. Each sampling, both for rainwater collection and stemflow collection, consisted of one or more consecutive rain events. A rain event is originally defined as rains of at least 1 mm of water depth and preceded by a dry period of at least 12 h [25].

Stemflow was collected using hoses with a diameter of 4 cm cut longitudinally in half and firmly fixed and sealed with silicone around the trunk of the trees at a 45° inclination to conduct, by gravity, the flowing water to 20 L collectors [7,26]. The concentrations of anions (Cl^- , NO_3^- , SO_4^{2-} , PO_4^{3-}) and cations (Na^{2+} , K^+ , Ca^{2+} , Mg^{2+}) were determined for both rainwater and stemflow samples, which were obtained monthly from composite samples totaling 12 samples for each studied process.

For sampling, virgin plastic bottles of 300 mL were used, which were previously washed with deionized water to avoid material contamination. Rain samples presenting different characteristics from the usual ones, such as odor, color, turbidity, or foreign bodies in the sample, were discarded. After collection, the bottles were stored at 4 °C until the analysis. The determinations of chemical elements were quantified using the METROHM ECO IC liquid chromatograph at the Laboratory of Hydrometeorology of Water and Soils of São Paulo State University, Sorocaba campus. For this purpose, 100 mL aliquots were prepared and filtered through a 0.45 µm cellulose filter. Chromatographic determination was performed by injecting a mobile phase passing through an ion exchange column (stationary phase), and detection was carried out by electrical conductivity. The analytical columns used were IonPac AS11HC (4 mm) and CS12A (4 mm) for anions and cations, respectively.

For the detection of anions, an eluent solution of sodium carbonate (Na_2CO_3) (Na_2CO_3) and sodium bicarbonate (NaHCO_3) with concentrations of 0.3 mM and 2.7 mM, respectively, was used. For the detection of cations, an eluent solution of methanesulfonic acid ($\text{CH}_4\text{O}_3\text{S}$) at a concentration of 2.6 mM was employed. The analyses were conducted automatically by a computer using the Peaknet 6.0 software, and the results were obtained through a calibration curve with the specific standards of the equipment. Quality control of the results was ensured using the certified sample TROIS-94. Concentrations were determined by comparison with the specific standards of the equipment. Ion concentrations exceeding 10 ppm were diluted with ultrapure type I water to prevent damage to the ion exchange column and to ensure that the estimated values were closer to the actual values.

2.2. Nutrients Input

Nutrient inputs were calculated using the volume-weighted mean ion concentration over a cumulative one-month period for each species for twelve months. For the calculation of the average ion concentrations, the weighted average of the ion concentrations according to the corresponding month was used, as calculated by Equation (1):

$$\text{VWM} = \frac{\sum_{n=1}^i \text{Ci} \times \text{Vi}}{\sum_{n=1}^i \text{Vi}} \quad (1)$$

where VWM is the volume-weighted mean ion concentration [mg L^{-1}], Ci is the ion concentration in the stemflow or rain [mg L^{-1}], and Vi is the volume [mm] of the stemflow or rain, both referring to the corresponding months [2,18,26].

To obtain the depth (mm) of rainfall [P] and stemflow [Sy] corresponding to each month, Equations (3) and (4) were used, as observed below.

$$\text{Precipitation: } P[\text{mm}] = \frac{V}{A} \quad (2)$$

$$\text{Stemflow: } \text{Sy}[\text{mm}] = \frac{V_t}{A_{pc}} \quad (3)$$

where P is the rainfall [mm], V represents the accumulated volume in the rain gauge (L), and A denotes the area of the rain gauge (m^2). For Sy: V_t is the total volume (L), and A_{pc} is the canopy projection area (m^2).

2.3. Bark Properties and Morphology

The bark water absorption capacity (BWA) for each tree was determined under laboratory conditions. Bark samples were collected from each tree, resulting in a composite sample per species at approximately the DBH (diameter at breast height). The lateral and internal surfaces of the bark samples were sealed in the field using a layer of silicone so that, during the experiment, water would be absorbed only by the outer layer of the bark. Thus, the fresh weight of the samples was obtained. Considering that bark samples from different species likely contain varying levels of residual water, the samples were air-dried for a minimum period of 30 days until reaching a constant mass [2,18,27]. Subsequently, the bark samples were fully submerged in deionized water and weighed during the first 12 h and then weighed at 12 h intervals until having been submerged for 96 h. After each weighing, the samples were submerged in water again [18,27,28] until they reached a constant mass. The bark water absorption capacity [BWA, %] was calculated as follows:

$$\text{BWA}\% = \frac{S_m - D_m}{D_m} \times 100 \quad (4)$$

where S_m is the weight of a sample after the subsequent immersion stage [g], and D_m is the weight of the dry sample [g].

As for the bark water absorption rate (BWA_{rate}), it was obtained at the end of the experiment, representing the amount of water that the bark stored beyond the time needed for the maximum bark water absorption (Equation (6)) [18].

$$\text{BWA}_{\text{rate}} = \frac{\text{BWA}_f - \text{BWA}_i}{t} \quad (5)$$

where BWA_i is the initial bark water absorption, BWA_f is the final bark water absorption, and t corresponds to the total absorption time.

The morphology of the barks was analyzed considering the bark texture, average depth of furrows (DF), and number of furrows (NS) at breast height (1.30 m from the ground) for the observer. For texture, the bark was classified as (1) smooth bark, (2) scaly/exfoliating bark, and (3) furrowed bark [18] (Figure 1).



Figure 1. Bark texture of the 8 studied tree species.

The analysis of the average depth of bark furrows (DF) was obtained by averaging the depth at 3 different locations around the circumference of the trunk, as visualized with a caliper. As for obtaining the number of furrows (NF), the number of furrows present in a 5 cm² area of bark was quantified using a magnifying glass. These pieces of information were then extrapolated to the circumference of the tree trunk, and the total was divided

by the diameter at breast height. The standard deviation (σ) was applied to define the classes of DF and NF, which consisted of a uniform distribution as the results deviated from the central average. This allowed the definition of 3 classes (intervals) for each analyzed property, as shown in Table 2.

Table 2. Classes of average depth OF FURROWS (DF) and number of furrows (NF).

Classes	DF	NF
1	$\overline{DF} - \sigma$	$\overline{NF} - \sigma$
2	$DF - \sigma < DF < \overline{DF} + \sigma$	$\overline{NF} - \sigma < NF < \overline{NF} + \sigma$
3	$\overline{DF} + \sigma$	$\overline{NF} + \sigma$

2.4. Statistical Analyses

Descriptive statistics were combined with field observations for a deeper process-based understanding of the differential ion concentration in the stemflow and bark water absorption capacity. Data analysis and processing were conducted using the R software (version 4.4.2). Analysis of variance (ANOVA) followed by Tukey's test at a 5% probability level was conducted to analyze the behavior of ions concerning the bark morphology and bark water absorption rate. Canonical redundancy analysis (RDA) was applied to measure the degree of variability among the tree species, considering the measured nutrient inputs in the stemflow (response variable) conditioned by the bark water absorption capacities obtained throughout the experiment (explanatory variables). In the RDA, each canonical ordination axis corresponded to a direction in the multivariate dispersion of the average ion concentrations—VWM—assessed in the stemflow that was maximally related to a linear combination of the explanatory variables—BWA% [29]. A Monte Carlo permutation test was used to assess the significance of the eigenvalues of the first two canonical axes.

3. Results

3.1. Nutrients Input and Bark Absorbability

The results obtained reveal that rainwater becomes enriched with ions as it interacts with tree structures, highlighting the crucial importance of stemflow as a fundamental route for nutrient transport to the soil. Overall, the order of the ion concentrations in the rainwater was as follows: $\text{Ca}^{2+} > \text{Cl}^- > \text{NO}_3^- > \text{K}^+ > \text{SO}_4^{2-} > \text{Mg}^{2+} > \text{PO}_4^{3-} > \text{Na}^{2+}$, while in the stemflow, the respective order observed was follows: $\text{K}^+ > \text{Ca}^{2+} > \text{Cl}^- > \text{SO}_4^{2-} > \text{NO}_3^- > \text{PO}_4^{3-} > \text{Mg}^{2+} > \text{Na}^{2+}$ (Figure 2).

The average ion concentration in the stemflow for all the species was 5 times higher than rainfall, approximately. On average, for anions, there was an increase of 410% for Cl^- , 230% for NO_3^- , 474% for SO_4^{2-} , and 315% for PO_4^{3-} . Regarding cations, there was an increase of 960% for Na^{2+} , 1514% for K^+ , 87% for Ca^{2+} , and 420% for Mg^{2+} . The studied species exhibited varied trends regarding both anion and cation input. Higher concentrations of Cl^- were observed in *M. polymorphum*, while the highest input of NO_3^- was recorded in *P. echinata*. Regarding SO_4^{2-} and PO_4^{3-} , they were more pronounced in *S. parahyba*. For cations, *E. urograndis* showed the highest inputs of Na^{2+} and Mg^{2+} , while *L. leucocephala* had the highest input of K^+ . The highest input of Ca^{2+} was observed in *P. taeda*.

When analyzing how the different species behaved regarding bark water absorption (BWA%), a wide variation in results was noticed, ranging from 39.5% (*P. echinata*) to 130.6% (*M. polymorphum*) (Figure 3). *M. polymorphum*, *P. granulosum*, and *E. urograndis* exhibited the highest percentages of absorptivity compared to the others, suggesting that their barks have a greater capacity to absorb water in a given unit of time until reaching total saturation conditions. However, the bark of *P. echinata* showed the lowest absorptivity. It can be observed that in subsequent time intervals, the bark water absorption capacity of all the species increased, resulting in significant increases in water absorption, regardless of the species. Additionally, it is noted that the species exhibited variations in their absorptivity dynamics as the water absorption capacity increased. However, it is interesting to note that

for all the species, the bark tended to reach a point of stability in absorptivity over time. When evaluating the absorbability rate among the species, it is noted that *P. granulosum* exhibited the highest absorption rate, followed by *M. polymorphum*, while *P. echinata* showed the lowest BWA_{rate} among the species, as represented in Table 3.

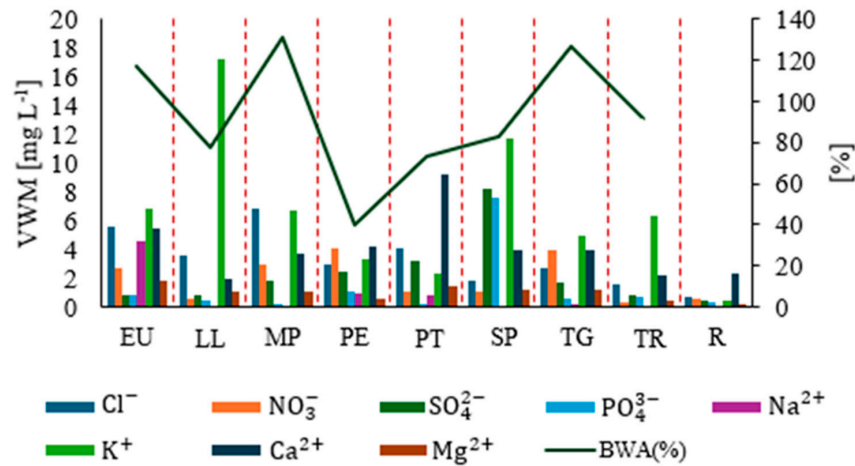


Figure 2. Volume-weighted mean [VWM, mg L⁻¹] in stemflow and rainfall [R, mg L⁻¹] for studied species and its relation to the bark storage capacity [BWA, %]. *E. urograndis* (EU), *L. leucocephala* (LL), *M. polymorphum* (MP), *P. echinata* (PE), *P. taeda* (PT), *S. parahyba* (SP), *T. granulosa* (TG), and *T. roseoalba* (TR).

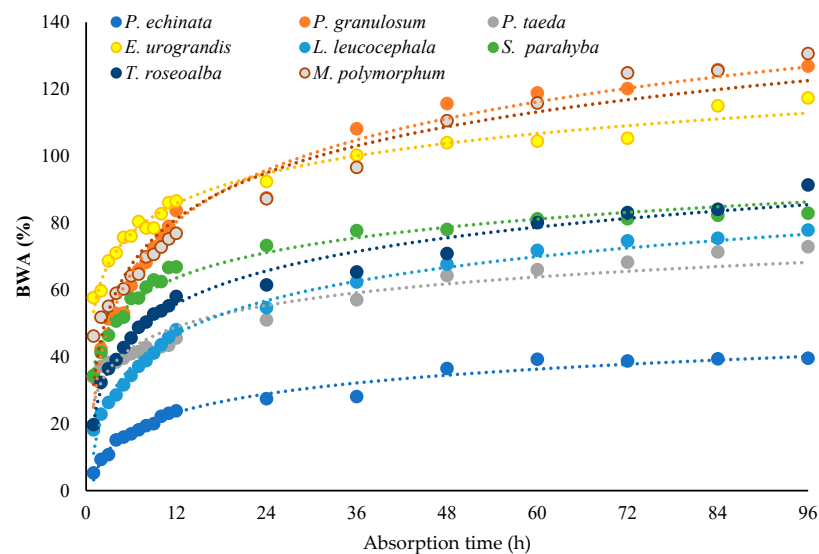


Figure 3. Bark water absorbability [BWA%] among studied tree species.

Table 3. Maximum bark water absorption capacity, BWA_{max} (%), and absorption rate, BWA_{rate} .

Species	BWA_{max} (%) ¹	BWA_{rate}
<i>E. urograndis</i>	117.35	0.62
<i>L. leucocephala</i>	77.85	0.62
<i>M. polymorphum</i>	130.62	0.88
<i>P. echinata</i>	39.52	0.36
<i>P. taeda</i>	72.88	0.40
<i>P. granulosum</i>	126.86	0.97
<i>T. roseoalba</i>	91.32	0.75
<i>S. parahyba</i>	82.92	0.51

¹ After 96 h of immersion.

3.2. Ion Concentrations, Morphology, and Bark Absorption Rate

The highest weighted mean concentrations (VWM) exhibited distinct behaviors among the classes of bark texture, depth, and number of furrows (Table 4). Considering bark texture, it was noted that rough bark showed the highest concentrations of Cl^- and NO_3^- , while scaly/bark exhibited higher levels of Na^{2+} , Ca^{2+} , and Mg^{2+} , and smooth bark recorded the highest concentrations of the ions SO_4^{2-} , PO_4^{3-} , and K^+ . However, only the concentrations of K^+ showed statistically significant differences among the bark texture classes. Regarding the bark water storage rate (BWA_{rate}), despite the fact that the species with furrowed bark exhibited a significant water absorption rate compared to those with other textures, no significant differences were observed.

Table 4. Weighted mean concentration (VWM) of anions and cations and absorption rate (BWA_{rate}) based on bark morphology. Values in parentheses correspond to standard error.

Class	Species ¹	Anions				Cations			Mg^{2+}	BWA_{rate}
		Cl^-	NO_3^-	SO_4^{2-}	PO_4^{3-}	Na^{2+}	K^+	Ca^{2+}		
Bark texture										
Furrowed	MP	6.84 a	2.93 a	1.88	0.19 a	0.04 a	6.67 ab	3.64 a	1.10 a	0.88 a
Scaly/Exfoliating	EU									
	PE	3.35 a	2.41 a	1.82 a	0.68 a	1.30 a	4.75 b	5.01 a	1.11 a	0.62 a
	PT	(0.69)	(0.75)	(0.47)	(0.13)	(0.83)	(0.87)	(0.16)	(0.26)	
	PG									
TR										
Smooth	LL	2.70 a	0.85 a	4.53 a	3.98 a	0.07 a	14.50 a	2.95 a	1.10 a	0.57 a
	SP	(0.86)	(0.24)	(3.72)	(3.58)	(0.03)	(2.77)	(1.03)	(0.04)	
Depth of Furrows in the bark										
<0.02	LL	2.70 a	0.85 a	4.53 a	3.98 a	0.07 a	14.50 a	2.95 a	1.10 a	0.57 a
	SP	(0.86)	(0.24)	(3.72)	(3.58)	(0.03)	(2.77)	(1.03)	(0.04)	
≥ 0.02 <0.10	EU	4.26 a	3.35 a	1.65 a	0.92 a	2.75 a	5.06 b	4.89 a	1.21 a	0.49 a
	PE	(1.35)	(0.67)	(0.82)	(0.12)	(1.80)	(1.76)	(0.62)	(0.63)	
≥ 0.10	MP									0.75 a
	PT	3.76 a	2.07 a	1.92 a	0.44 a	0.26 a	5.07 b	4.73 a	1.04 a	
	PG	(1.02)	(0.75)	(0.44)	(0.11)	(0.16)	(0.89)	(1.36)	(0.19)	
	TR									
Number of furrows in the bark										
<10	LL	2.70 a	0.85 a	4.53 a	3.98 a	0.07 a	14.50 a	2.95 a	1.11 a	0.57 ab
	SP	(0.86)	(0.24)	(3.72)	(3.58)	(0.03)	(2.77)	(1.03)	(0.04)	
≥ 10.12 <50.28	PE	3.47 a	2.53 a	2.87 a	0.65 a	0.86 a	2.80 b	6.71 a	0.99 a	0.38 b
	PT	(0.55)	(1.49)	(0.37)	(0.39)	(0.08)	(0.50)	(2.44)	(0.42)	
≥ 50.28	EU									0.81 a
	MP	4.16 a	2.48 a	1.31 a	0.58 a	1.20 a	6.20 a	3.82 a	1.15 a	
	PG	(0.11)	(0.69)	(0.26)	(0.12)	(1.00)	(0.39)	(0.61)	(0.26)	
	TR									

¹ E. urograndis (EU), L. leucocephala (LL), M. polymorphum (MP), P. echinata (PE), P. taeda (PT), S. parahyba (SP), T. granulosa (TG), and T. roseoalba (TR).

The highest water storage rate was associated with $DF \geq 0.10$. However, it is important to highlight that the highest concentrations of the ions were associated with DF values <0.02 and $\geq 10.12 < 50.28$. Specifically, when analyzing the ions, it is noticeable that the barks with a shallower depth (<0.02 mm) exhibited higher concentrations of SO_4^{2-} , PO_4^{3-} , and K^+ . However, no statistical differences were observed among the ions, except for the concentration of K^+ between the bark with a shallower depth and the others.

The BWA rate values and the highest concentrations of Cl^- , Na^{2+} , and Mg^{2+} were associated with barks with deeper furrows (≥ 50.28). On the other hand, the barks with a lower number of furrows (<10) showed higher concentrations of SO_4^{2-} , PO_4^{3-} , and K^+ . However, a statistically significant difference was observed only for the concentrations of K^+ , where the classes with fewer and greater numbers of furrows were similar.

Considering the bark texture, depth, and number of furrows, SO_4^{2-} , PO_4^{3-} , and K^+ were similar for bark texture, furrow depth, and number of furrows, with the highest concentrations being observed in the smooth bark species, with $DF < 0.02$ and $NF < 0.10$, as represented by *L. leucocephala* and *S. parahyba*. On the other hand, Na^{2+} and Mg^{2+} had higher concentrations in the species with an exfoliating texture (*E. urograndis*, *P. echinata*, *P. taeda*, *P. granulosum*, *T. roseoalba*), with $DF > 0.02 \leq 0.10$ (*E. urograndis*; *P. echinata*) and $NF > 50.28$ (*E. urograndis*, *M. polymorphum*, *P. granulosum*, *T. roseoalba*), in which *E. urograndis* was present in all classes. The other ions had different behaviors among the analyzed classes. The anions Cl^- and NO_3^- had the highest concentrations in furrowed bark species (*M. polymorphum*) and had $DF > 0.02 \leq 0.10$ (*E. urograndis*; *P. echinata*); however, they were different in terms of NF , where for Cl^- , it corresponded to $NF \geq 50.28$ (*E. urograndis*, *M. polymorphum*, *P. granulosum*, *T. roseoalba*), and for NO_3^- , it corresponded to $NF > 10.12 \leq 50.28$, as represented by the species *P. taeda* and *P. echinata*.

The ion Ca^{2+} was found in higher concentrations in species with a scaly/exfoliating texture (*E. urograndis*, *P. echinata*, *P. taeda*, *P. granulosum*, *T. roseoalba*), with $DF \geq 0.02 < 0.10$ (*E. urograndis*, *P. echinata*) and $NF > 10.12 \leq 50.28$ (*P. taeda* and *P. echinata*), where it is worth noting that *P. echinata* was the only species that remained in all three defined classes. The highest water storage rate corresponded to *M. polymorphum*, which is represented by a furrowed texture. As for DF , it equated to ≥ 0.10 , as composed of the species *M. polymorphum*, *P. taeda*, *P. granulosum*, and *T. roseoalba*, and $NF \geq 50.28$ (*E. urograndis*, *M. polymorphum*, *P. granulosum*, *T. roseoalba*). It is worth noting that *M. polymorphum* was the only species that was grouped in the same analyzed classes (bark texture, depth, and number of furrows), while the others had a differentiated distribution among the classes.

Canonical redundancy analysis (RDA) was used to investigate the factors influencing the species data variation and bark water absorption capacity (Figure 4). The analysis showed that the concentration of ions in the stemflow significantly explained the variability in the species data (p -value < 0.05). Specifically, the variable BWA% accounted for 15.6% of the adjusted R value, elucidating the variation in the ion concentration in the stemflow. This result highlights the significance of ion concentrations in influencing both species data and bark's water absorption. The direction and length of the vectors (in blue) indicate the direction and magnitude of the explanatory variable's influence in the canonical space (axes), so the proximity of the points to the vectors indicates how the explanatory variables affect the observations. Based on the results, four trends were observed, where the BWA% for *S. parahyba* was strongly influenced by PO_4^{3-} and SO_4^{2-} , while the bark absorption capacity of *E. urograndis* and *P. taeda* was related to the ions Cl^- , Na^{2+} , Ca^{2+} , and Mg^{2+} . When evaluating the BWA% of *M. polymorphum*, *P. granulosum*, and *T. roseoalba*, a positive influence for the NO_3^- ion was observed. However, it was not possible to identify the predominant influence on the BWA% for *P. echinata*.

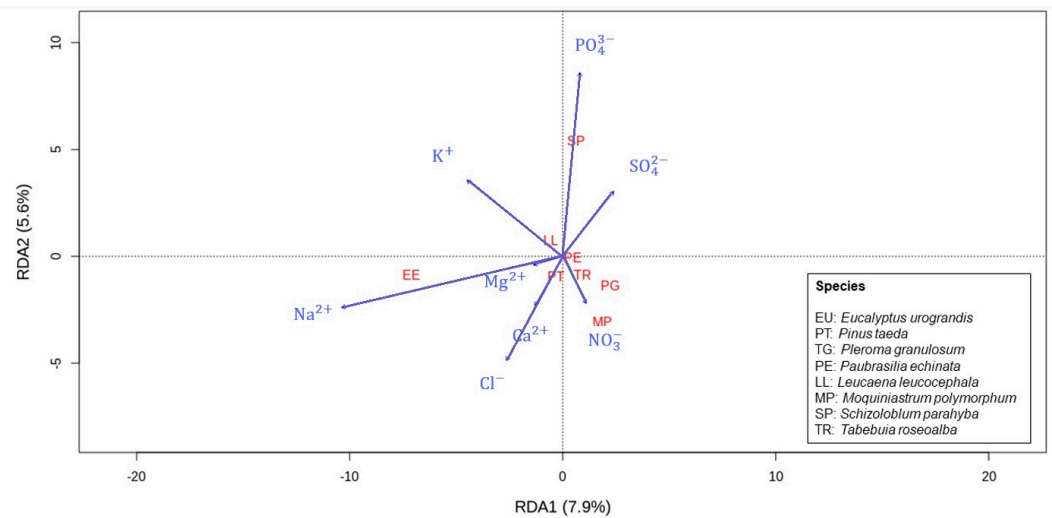


Figure 4. Ordination diagram of the RDA analysis of bark absorption capacity (BWA%) of species, with ion variables shown as arrows. The ions Cl^- , NO_3^- , SO_4^{2-} , PO_4^{3-} , Na^{2+} , K^+ , Ca^{2+} , and Mg^{2+} represent VWM values contained in the stemflow.

4. Discussion

There is a dynamic interaction between bark and water, in which bark plays a fundamental role in the exchange of both inorganic and organic ions with rainwater, either throughfall or stemflow [3]. It is of paramount importance to predict how the morphological characteristics of bark and its water absorption affect the behavior of ion release, either through the leaching or adsorption of ions contained in the bark of the tree species.

In addition to the morphometric characteristics of bark, its internal structure can play a significant role in affecting its water absorption capacity. In this investigation, it was suggested that the leaching rates of Mg^{2+} and Ca^{2+} may be influenced by the thickness of the rhytidome and periderm [30]. This study corroborated that Ca^{2+} , along with Cl^- , was more associated with the BWA% of the species that had a thicker bark texture (*P. taeda*). On the other hand, Mg^{2+} , as well as Na^{2+} , was influenced by the BWA% of the species *E. urograndis*, which, in turn, does not have thick rhytidome and periderm. However, it is very common in *Eucalyptus* sp. for old layers of bark—outer bark or rhytidome—to peel off, which may influence the release of Mg^{2+} as well as the ion Na^{2+} . Previous studies [31] have confirmed that thinner layers of dead tissue, which commonly cover younger branches and tree trunks, allow some ion mobility between the closer functional internal tissues and the bark.

Furthermore, our results suggested that the leaching rates of K^+ seem to be driven by the presence of cellular structures associated with resource storage (parenchyma) and transfer (sieve cells) [30], which, in turn, is consistent with the RDA results for the BWA% of the species *L. leucocephala*, where potassium was the most influenced by the bark absorption capacity. Researchers studying *L. leucocephala*, *Bauhinia cheilantha*, and *Mimosa caesalpinifolia* observed that the abaxial epidermis was thinner than the adaxial one, and the stomata on the abaxial surface were numerous, with the palisade parenchyma juxtaposed, arranged in a single layer with few intercellular spaces [32]. The presence of K^+ is the result of the leaching of this ion from the canopy itself [33]. The high susceptibility of K^+ can be attributed to its easy mobility [1,34]. Thus, as supported by previous studies, it can be inferred that potassium can easily move within plants and be released into the stemflow.

In RDA, the percentage of variation explained by the canonical axes helps to understand how much of the total variation in the dependent variables is captured by the axes. In this way, the results suggest a low association (RDA 7.9 and 5.6) between the bark absorption capacity and the ion concentration. Therefore, it can be inferred that not only is bark's water absorption capacity necessarily related to ion leaching, but it may also be

influenced by atmospheric deposition as well as other factors. The nutrient concentration is the result of internal canopy processes, either through canopy leaching and/or through external processes, and it is affected by the washing of ions deposited on trees.

The anatomical structure of the bark of different tree species can also be a very important factor that affects its water storage capacity; however, this was not the subject of the present study [27]. Recent studies suggest that the anatomical characteristics of bark are related to the chemistry of the stemflow for ions of commonly leached macronutrients (K^+ , Mg^{2+} , and Ca^{2+}) in a wide variety of bark types of coniferous and deciduous tree species [30].

It is known that barks have a chemical composition, structural components, and organic and inorganic accidental components in their structures. In terms of structural components, there are cellulose, hemicelluloses, and lignin. Lignin is a polyphenolic material, highly branched, three-dimensional, and amorphous, which provides rigidity to the cell wall and also acts as a permanent bonding agent between cells [35]. An investigation conducted in the outer bark of the Brazilian Cerrado species showed that wetness, the lignin content, and stemflow yields were not associated with lignin, and they also did not influence the bark's water absorbability process [18].

One of the objectives of this study was to characterize the ion concentration in the stemflow as a function of the bark morphology based on texture classes, depth, and number of furrows. Specifically, regarding the bark absorption rate, it is evident that the results were related to species with a furrowed texture, a greater depth, and a higher number of furrows. The observed differences in the normative water storage capacity of the bark in the studied species (*Betula lenta*, *Carya glabra*, *Quercus rubra*) can be attributed to variations in bark roughness, bark morphology, and water behavior on bark surfaces. In this study, a greater bark roughness was consistent with higher normative water retention capacities in the bark [13].

However, when analyzing the ion concentrations based on the bark morphology results, it is noted that they failed to transcribe how these variables were related to each other. For example, when examining species characterized with smooth bark, a shallower depth, and fewer furrows, they recorded higher concentrations of PO_4^{3-} , SO_4^{2-} , and K^+ . Among this group were *L. leucocephala* and *S. parahyba*, with the former recording the lowest concentrations of PO_4^{3-} and SO_4^{2-} , in contrast to *S. parahyba*, although both indeed showed the highest concentrations of K^+ . In this case, indeed, these smooth-barked species confirm the attribution of K^+ being easily leached from plant structures. If atmospheric deposition was the primary source of K^+ , it would be expected that its highest concentration would be in the stemflow from species with rougher bark due to the larger contact surface compared to trees with smoother bark.

Still, the concentrations of Cl^- and NO_3^- were found to be higher in furrowed barks (in the case of *M. polymorphum*). This information contributes to Cl^- being justified even by the higher amount of dead tissue in rough barks that, when interacting with water, is dissolved and carried away by the stemflow [36]. The results of the RDA showed that the NO_3^- ion was strongly related to the water absorption capacity of *M. polymorphum*'s bark. However, the highest concentrations of NO_3^- were associated with *P. echinata*, which has bark in scale/exfoliative form. The same reasoning can also be applied when comparing the other morphological classes of bark.

It is known that species with rough-textured bark experience longer water retention times from stemflow on the bark, a factor that favors ion exchange between the bark and the aqueous environment, consequently leading to the leaching of ions present in the bark [25]. Although studies indicate that ions present in stemflow are more concentrated in species with rough bark than in species with smooth bark, the results showed that species with smooth bark had higher concentrations compared to other species with furrowed characteristics, suggesting that there are other variables influencing the nutrient flux. Therefore, it is emphasized that the findings above have important implications for understanding the interaction processes between trees and the environment, especially

in terms of nutrient cycling and tree responses to different environmental conditions. However, it is clear that we cannot generalize the potential for the enrichment of ion concentrations in stemflow solely based on bark morphology and bark water absorption capacity. In addition to other biotic characteristics that were not measured in this study, there are various abiotic factors involved that must be considered in the process of nutrient enrichment in stemflow, such as the wind direction as well as aerosol sources near the study area. Thus, there is a need for further research to fully understand how tree bark characteristics influence these processes.

5. Conclusions

The results of this study underscore the importance of studying the intricate relationship between bark characteristics, stemflow, and nutrient flux, revealing a nuanced interaction between the physical and chemical properties of the bark and the nutrient composition of water traversing the stemflow. Our analysis of the ion concentration in the stemflow relative to the bark's water absorption capabilities highlighted significant variations among species characterized by furrowed textures, an increased depth, and a higher number of furrows. Despite these insights, our examination of how the bark morphology—categorized by texture, depth, and number of furrows—influences these processes remained inconclusive. The canonical redundancy analysis (RDA) indicated a modest correlation between the bark absorption capacity and ion concentration, suggesting that factors beyond the immediate scope of this study, potentially external environmental variables or other unexplored bark characteristics, may play a pivotal role in ion leaching dynamics. This underscores the complexity of the ecohydrological processes at play and points to the necessity for further research to disentangle the myriad factors influencing nutrient transport in urban tree ecosystems.

Author Contributions: Methodology, M.T.L. and K.C.T.; formal analysis, K.C.T.; investigation, M.T.L., M.E.G.G. and K.C.T.; writing—original draft, M.T.L.; writing—review and editing, K.C.T.; supervision, K.C.T. All authors have read and agreed to the published version of the manuscript.

Funding: This research was funded by the Brazilian National Council for Scientific and Technological Development (CNPq), Coordenação de Aperfeiçoamento de Pessoal de Nível Superior—Brasil (CAPES)—finance code 001 and the São Paulo Research Foundation (FAPESP), grant 2021/11697-9.

Data Availability Statement: The data that support the findings of this study are available from the corresponding author upon reasonable request.

Conflicts of Interest: The authors declare no conflicts of interest.

References

1. Momolli, D.R.; Schumacher, M.V.; Viera, M.; Ludvichak, A.A.; Guimarães, C.D.C.; Souza, H.P.D. Incident Precipitation Partitioning: The Canopy Interactions Enrich Water Solution with Nutrients in Throughfall and Stemflow. *J. Agric. Sci.* **2019**, *11*, 351. [[CrossRef](#)]
2. Sun, X.; Zhang, Z.; Cao, Y.; Liu, L.; Hu, F.; Lu, X. Canopy Modification of Base Cations Deposition in a Subtropical Broadleaved Forest: Spatial Characteristics, Canopy Budgets and Acid Neutralizing Capacity. *Ecol. Manag.* **2021**, *482*, 118863. [[CrossRef](#)]
3. Van Stan, J.T.; Dymond, S.F.; Klamerus-Iwan, A. Bark-Water Interactions Across Ecosystem States and Fluxes. *Front. For. Glob. Chang.* **2021**, *4*, 660662. [[CrossRef](#)]
4. Van Stan, J.T.; Allen, S.T. What We Know About Stemflow's Infiltration Area. *Front. For. Glob. Chang.* **2020**, *3*, 61. [[CrossRef](#)]
5. Carlyle-Moses, D.E.; Iida, S.; Germer, S.; Llorens, P.; Michalzik, B.; Nanko, K.; Tischer, A.; Levia, D.F. Expressing Stemflow Commensurate with Its Ecohydrological Importance. *Adv. Water Resour.* **2018**, *121*, 472–479. [[CrossRef](#)]
6. Astuti, H.P.; Suryatmojo, H. Water in the forest: Rain-vegetation interaction to estimate canopy interception in a tropical borneo rainforest. *IOP Conf. Ser. Earth Environ. Sci.* **2019**, *361*, 012035. [[CrossRef](#)]
7. Schooling, J.T.; Levia, D.F.; Carlyle-Moses, D.E.; Dowtin, A.L.; Brewer, S.E.; Donkor, K.K.; Borden, S.A.; Grzybowski, A.A. Stemflow Chemistry in Relation to Tree Size: A Preliminary Investigation of Eleven Urban Park Trees in British Columbia, Canada. *Urban. Urban. Green.* **2017**, *21*, 129–133. [[CrossRef](#)]
8. Zhang, Y.F.; Wang, X.P.; Pan, Y.X.; Hu, R. Variations of Nutrients in Gross Rainfall, Stemflow, and Throughfall Within Revegetated Desert Ecosystems. *Water Air Soil. Pollut.* **2016**, *227*, 183. [[CrossRef](#)]
9. Tonello, K.C.; Rosa, A.G.; Pereira, L.C.; Matus, G.N.; Guandique, M.E.G.; Navarrete, A.A. Rainfall Partitioning in the Cerrado and Its Influence on Net Rainfall Nutrient Fluxes. *Agric. Meteorol.* **2021**, *303*, 108372. [[CrossRef](#)]

10. Aubrey, D.P.; Van Stan, J.T.; Gutmann, E.; Friesen, J. *Relevance of Precipitation Partitioning to the Tree Water and Nutrient Balance Precipitation Partitioning by Vegetation: A Global Synthesis*; Springer: Cham, Switzerland, 2020.
11. Germer, S.; Zimmermann, A.; Neill, C.; Krusche, A.V.; Elsenbeer, H. Disproportionate Single-Species Contribution to Canopy-Soil Nutrient Flux in an Amazonian Rainforest. *Ecol. Manag.* **2012**, *267*, 40–49. [[CrossRef](#)]
12. Levia, D.F.; Frost, E.E. A Review and Evaluation of Stemflow Literature in the Hydrologic and Biogeochemical Cycles of Forested and Agricultural Ecosystems. *J. Hydrol.* **2003**, *274*, 1–29. [[CrossRef](#)]
13. Levia, D.F.; Herwitz, S.R. Interspecific Variation of Bark Water Storage Capacity of Three Deciduous Tree Species in Relation to Stemflow Yield and Solute Flux to Forest Soils. *Catena* **2005**, *64*, 117–137. [[CrossRef](#)]
14. Chuyong, G.B.; Newbery, D.M.; Songwe, N.C. Rainfall Input, Throughfall and Stemflow of Nutrients in a Central African Rain Forest Dominated by Ectomycorrhizal Trees. *Biogeochemistry* **2004**, *67*, 73–91. [[CrossRef](#)]
15. Oka, A.; Takahashi, J.; Endoh, Y.; Seino, T. Bark Effects on Stemflow Chemistry in a Japanese Temperate Forest I. The Role of Bark Surface Morphology. *Front. For. Glob. Chang.* **2021**, *4*, 654375. [[CrossRef](#)]
16. Song, Q.N.; Lu, H.; Liu, J.; Yang, J.; Yang, G.Y.; Yang, Q.P. Accessing the Impacts of Bamboo Expansion on NPP and N Cycling in Evergreen Broadleaved Forest in Subtropical China. *Sci. Rep.* **2017**, *7*, 40383. [[CrossRef](#)] [[PubMed](#)]
17. Van Stan, J.T.; Levia, D.F. Inter- and Intraspecific Variation of Stemflow Production from *Fagus Grandifolia* Ehrh. (American Beech) and *Liriodendron Tulipifera* L. (Yellow Poplar) in Relation to Bark Microrelief in the Eastern United States. *Ecohydrology* **2010**, *3*, 11–19. [[CrossRef](#)]
18. Tonello, K.C.; Campos, S.D.; Menezes, A.J.; Bramorski, J.; Mathias, S.L.; Lima, M.T. How Is Bark Absorbability and Wettability Related to Stemflow Yield? Observations From Isolated Trees in the Brazilian Cerrado. *Front. For. Glob. Chang.* **2021**, *4*, 650665. [[CrossRef](#)]
19. Tobon Marin, C.; Bouten, I.W.; Dekker, S. Forest Floor Water Dynamics and Root Water Uptake in Four Forest Ecosystems in Northwest Amazonia. *J. Hydrol.* **2000**, *237*, 169–183. [[CrossRef](#)]
20. Shearman, T.M.; Varner, J.M. Variation in Bark Allocation and Rugosity Across Seven Co-Occurring Southeastern US Tree Species. *Front. For. Glob. Chang.* **2021**, *4*, 731020. [[CrossRef](#)]
21. Crockford, R.H.; Richardson, D.P. Partitioning of Rainfall into Throughfall, Stemflow and Interception: Effect of Forest Type, Ground Cover, and Climate. *Hydrol. Process.* **2000**, *14*, 2903–2920. [[CrossRef](#)]
22. Siegert, C.; Ilek, A.; Wade, A.; Schweitzer, C. Changes in Bark Properties and Hydrology Following Prescribed Fire in *Pinus Taeda* and *Quercus Montana*. *Hydrol. Process* **2023**, *37*, e14799. [[CrossRef](#)]
23. Dubreuil, V.; Fante, K.P.; Planchon, O.; Sant’Anna Neto, J.L. Climate Change Evidence in Brazil from Köppen’s Climate Annual Types Frequency. *Int. J. Climatol.* **2019**, *39*, 1446–1456. [[CrossRef](#)]
24. Santos, H.G.; Jacomine, P.K.T.; Anjos, L.H.C.; Oliveira, V.A.; Lumbreras, J.F.; Coelho, M.R.; Almeida, J.A.; Araujo Filho, J.C.; Oliveira, J.B.; Cunha, T.J.F. *Sistema Brasileiro de Classificação de Solos*; Embrapa Solos: Brasília, Brazil, 2018.
25. André, F.; Jonard, M.; Ponette, Q. Effects of Biological and Meteorological Factors on Stemflow Chemistry within a Temperate Mixed Oak-Beech Stand. *Sci. Total Environ.* **2008**, *393*, 72–83. [[CrossRef](#)] [[PubMed](#)]
26. Hofhansl, F.; Wanek, W.; Drage, S.; Huber, W.; Weissenhofer, A.; Richter, A. Controls of Hydrochemical Fluxes via Stemflow in Tropical Lowland Rainforests: Effects of Meteorology and Vegetation Characteristics. *J. Hydrol.* **2012**, *452–453*, 247–258. [[CrossRef](#)]
27. Klammerus-Iwan, A.; Lasota, J.; Błońska, E. Interspecific Variability of Water Storage Capacity and Absorbability of Deadwood. *Forests* **2020**, *11*, 575. [[CrossRef](#)]
28. Ilek, A.M.; Kucza, J.; Morkisz, K. Hydrological Properties of Bark of Selected Forest Tree Species. Part 2: Interspecific Variability of Bark Water Storage Capacity. *Folia For. Pol. Ser. A* **2017**, *59*, 110–122. [[CrossRef](#)]
29. Leps, J. *Multivariate Analysis of Ecological Data Using CANOCO*; Cambridge University Press: Cambridge, UK, 2003.
30. Oka, A.; Takahashi, J.; Endoh, Y.; Seino, T. Bark Effects on Stemflow Chemistry in a Japanese Temperate Forest II. The Role of Bark Anatomical Features. *Front. For. Glob. Chang.* **2021**, *4*, 657850. [[CrossRef](#)]
31. Legrand, I.; Asta, J.; Goudard, Y. Variations in Bark Acidity and Conductivity over the Trunk Length of Silver Fir and Norway Spruce. *Trees* **1996**, *11*, 54–58. [[CrossRef](#)]
32. Silva, M.A.; dos Santos, M.V.F.; Lira, M.A.; Dubeux Júnior, J.C.B.; de Andrade Silva, D.K.; Santoro, K.R.; de Arruda Leite, P.M.B.; de Freitas, E.V. Qualitative and Anatomical Characteristics of Tree-Shrub Legumes in the Forest Zone in Pernambuco State, Brazil. *Rev. Bras. Zootec.* **2012**, *41*, 2396–2404. [[CrossRef](#)]
33. Rodrigo, A.; Ávila, A.; Rodà, F. The Chemistry of Precipitation, Throughfall and Stemflow in two Holm Oak (*Quercus ilex* L.) Forests under a Contrasted Environment in NE Spain. *Sci. Total Environ.* **2003**, *305*, 195–205. [[CrossRef](#)]
34. Tóbon, C.; Sevink, J.; Verstraten, J.M. Solute Fluxes in Throughfall and Stemflow in Four Forest Ecosystems in Northwest. *Biogeochemistry* **2004**, *70*, 1–25. [[CrossRef](#)]
35. García Hortal, J.A. *Fibras Papeleras*; Edicions PC: Barcelona, Spain, 2007; 243p.
36. Su, L.; Zhao, C.; Xu, W.; Xie, Z. Hydrochemical Fluxes in Bulk Precipitation, Throughfall, and Stemflow in a Mixed Evergreen and Deciduous Broadleaved Forest. *Forests* **2019**, *10*, 507. [[CrossRef](#)]

Disclaimer/Publisher’s Note: The statements, opinions and data contained in all publications are solely those of the individual author(s) and contributor(s) and not of MDPI and/or the editor(s). MDPI and/or the editor(s) disclaim responsibility for any injury to people or property resulting from any ideas, methods, instructions or products referred to in the content.